Advances in Differential Equations and Control Processes 2025, 32(1), 2807.
https://doi.org/10.59400/adecp2807

Article

Performance evaluation of post-processed kinematic precise point positioning solution for environmental applications

Ahmed Al Shouny

Department of Geomatics, King Abdulaziz University, Jeddah 21589, Saudi Arabia; ametaowa@kau.edu.sa

CITATION

Al Shouny A. Performance evaluation of post-processed kinematic precise point positioning solution for environmental applications. Advances in Differential Equations and Control Processes. 2025; 32(1): 2807. https://doi.org/10.59400/adecp2807

ARTICLE INFO

Received: 18 February 2025
Accepted: 7 March 2025
Available online: 13 March 2025

Abstract: Precise Point Positioning (PPP) is a modern satellite-based technique known for its simplicity, efficiency, and cost-effectiveness, eliminating the need for a reference or base station. This study evaluates the accuracy of Precise Point Positioning (PPP) solutions for both static and kinematic observations using the CSRS-PPP service. To ensure a fair comparison, PPP-derived results were assessed against relative positioning techniques. Field measurements, including static and kinematic data, were collected across a 39 km² study area in northern Egypt to generate topographic contour maps. The findings indicate that PPP is a viable alternative for static positioning, achieving a 2D horizontal accuracy of ±2.54 cm, though vertical accuracy is lower at 11.3 cm. In kinematic mode, horizontal accuracy is ±5 cm, while vertical accuracy decreases to 18.4 cm. While the achieved 2D accuracy meets the needs of most environmental applications, the lower height precision may not be suitable for tasks requiring high vertical accuracy.

Keywords: post-processed kinematic PPP; CSRS-PPP; relative positioning; static measurements

1. Introduction

Differential GNSS (DGNSS) using carrier phase observations has become widely used across various fields, offering centimeter-level accuracy in both static and kinematic modes. However, it requires at least two GNSS receivers—one as a base and one as a rover—operating simultaneously. For high-accuracy applications like geodesy, static and rapid static methods are preferred, achieving millimeter-level precision [1] but requiring extended measurement and processing time which could limit its applications [2,3]. Kinematic methods, while slightly less accurate, are widely used in several applications such as land surveying, mapping, construction, border, aircraft positioning, mining, agriculture, and marine works [4]. Initially, Post-Processed Kinematic (PPK) was the only available solution for kinematic GPS data, but Real-Time Kinematic (RTK) was later introduced, providing instant corrections through continuous radio communication. RTK has since become a crucial tool due to its speed, accuracy, and cost-effectiveness.

Both static and kinematic relative positioning techniques have limitations that restrict their use in various applications and regions. The requirement of at least two receivers for simultaneous measurement increases fieldwork complexity and time. A major challenge is the scarcity of reference points, especially in remote and coastal areas [5]. Static mode requires lengthy installation and post-processing, making it impractical for some applications. RTK is limited by a maximum base-rover separation of 20 km [6], which affects ambiguity resolution for centimeter-level

accuracy. Additionally, RTK connections are prone to signal interruptions due to physical obstructions, interference, or environmental conditions.

Over several years, researchers and scientists perform many studies to develop new techniques and approaches to overcome the above-mentioned limitations of relative positioning methods. These approaches include Continuously Operating Reference Station (CORS), the Virtual Reference Station (VRS) [7], and Precise Point Positioning (PPP). PPP has been considered one of the most popular positioning approaches in recent years. The development of the PPP technique was a result of the precise GPS clock and orbit products provided by the International Global Navigation Satellite System (GNSS) service (IGS) organization. PPP can process observations collected by single or dual-frequency receivers using both static and kinematic methods [8]. Thanks to IGS products, PPP can achieve cm-level accuracy without the need for using reference stations [9]. So PPP is considered easier and less expensive than relative positioning techniques, and therefore it has become the most widely used approach for several scientific and practical fields.

The obtained accuracies of the PPP solution for static and kinematic methods in various applications have been investigated in several studies [10–15]. They have concluded that PPP for static mode can achieve mm to cm level accuracy in positions. However, in kinematic mode, PPP can achieve centimeters to a few decimeters in positions [5,12,16–18]. According to numerous research investigations, it was concluded that PPP vertical error is about twice the value of the PPP horizontal errors [5,19,20]. The different available services and software of PPP were assessed and compared in several studies. The Canadian Spatial Reference System Precise Point Positioning (CSRS-PPP) service concluded as the most accurate PPP service [11,12,21–23].

This study evaluates PPP accuracy for both static and kinematic measurements using the CSRS-PPP service and compares the results with relative positioning techniques. The adaptation of the PPP kinematic mode in environmental applications is examined to assess its obtained accuracy in horizontal and vertical components. The study area covering approximately 39 km^2 is placed alongside the Mediterranean Sea coast in the northern region of Egypt. The choice of this coastal area is because of its significance in continuous construction and development projects that led to the permanent need for coastal protection strategies and works to fight erosion caused by global warming. Additionally, the area's unique geographical and climatic conditions, such as high humidity, temperature variations, and potential ionospheric disturbances, may influence GNSS positioning accuracy. Another key factor in selecting this coastal region is due to the severe shortage of reference points in most of the coastal areas. This paper is organized as follows. First, a brief discussion of relative positioning and PPP techniques and their mathematical models is presented. Second, the study area and field measurements are discussed. Next, the results are presented, compared, and analyzed. Finally, the conclusions of the paper were introduced.

2. Relative positioning and PPP techniques

Relative positioning methods, also known as differential positioning techniques, are considered the most accurate techniques for the estimation of positions in both

horizontal and vertical components. Static and rapid static are used for geodetic and surveying applications that require the highest accuracy. However, they need a long time of observations and also a post-processing stage. For long baselines, only the static method is applicable for observations. Kinematic methods include both PPK and RTK. RTK provides positions instantaneously by receiving corrections from the base units via radio connection. Unlike static methods, RTK does not require post-processing, and its achieved accuracy is less than static accuracy, but it can achieve an acceptable accuracy up to cm-level accuracy [24]. PPK can provide more accuracy than RTK as a result of the post-processing stage that removes data blunders and errors [4]. PPK can provide us with cm-accuracy after solving ambiguity [1]. PPK, unlike RTK, can't provide positions in real time. PPK needs less occupation time than static and rapid static methods. However, it requires initialization time at the beginning of the observing process and after losing the satellite signals. This initialization process is essential for solving ambiguity. The PPK method consists of two primary modes. The first is the continuous mode, where the rover remains in motion, making it ideal for applications such as railway surveys and GPS-controlled photogrammetry. The second mode, which we employed in this study, is the stop-and-go mode. In this approach, the rover briefly pauses at each unknown point for less than two minutes. Compared to the continuous mode, stop-and-go surveying offers higher accuracy and is better suited for contour and detail surveys. This is because data can be averaged over the collection period at each site, reducing uncertainty and improving positional accuracy by minimizing errors when the receiver remains stationary at designated points [4]. The estimation of positions by relative positioning using the double differencing principle in phase measurements is calculated by equation [25]:

$$\nabla\Delta\phi_t = \nabla\Delta r_{(t,t-\tau)} + \nabla\Delta ds_{(t-\tau)} - \nabla\Delta d_{iono} + \nabla\Delta d_{tropo} + \nabla\Delta\lambda N + \nabla\Delta\varepsilon(\phi) \quad (1)$$

where: $\nabla\Delta$ is the double difference operator at the time of receiving data (t), ϕ is the phase measurement, τ is the travel time from satellite to receiver, $t-\tau$ is the satellite time, $r_{(t,t-\tau)}$ refers to the true geometric range, ds is the orbital prediction error, d_{iono} and d_{tropo} are the ionospheric and tropospheric errors, respectively, λ is the wavelength, N is the integer phase ambiguity, and ε denotes the noise component. The tropospheric delay is the sum of the wet and hydrostatic parts.

Due to the extensive use of GNSS in a variety of applications and fields, it was necessary for researchers and organizations to develop new strategies and techniques. The main concern of these strategies is to be simpler, cost-effective, widely popular, and to achieve an acceptable accuracy compared with traditional relative positioning techniques. One of these modes developed strategies is PPP techniques. PPP was first introduced and discussed by [9]. It was first developed for static works only but later, with the availability of precise real-time satellite orbit and clock products provided by the IGS organization. It was adopted in kinematic applications [16]. PPP is considered the most popular used GNSS technique in scientific research and several applications. PPP is also known as Single Point Positioning (SPP), as it used only one receiver without the need for reference point occupation, as shown in **Figure 1**. Not only is PPP simple and cost-effective with global coverage, but it also achieves an acceptable accuracy in static and kinematic modes. PPP solutions can be obtained using either

web-based online services or different software/web-based online services such as MAGIC-GNSS, Automatic Precise Positioning Service (APPS), Trimble CenterPoint (RTX), GNSS Analysis and Positioning Software (GAPS), and CSRS-PPP. Regarding software, they are divided into two categories: Scientific software (GipsyX, GAMIT, GLAB, and the most popular one) and commercial software (GRAF-NAV) [26].

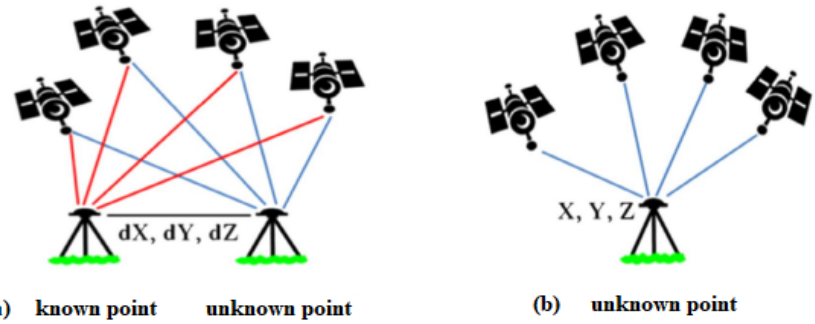

Figure 1. Schematic depicting **(a)** relative positioning; and **(b)** point positioning.

In this study, CSRS-PPP online service is considered the globally used popular PPP service [27]. It can process both static and kinematic data with no charge, and this service provides registered users with a PDF file containing results and graphical information of the processing solution. Full explanation and details of the CSRS-PPP service were introduced by [28–30]. It should be noted that one of the most important parts of the PPP technique is the solution type of initial phase ambiguities, which can be fixed or float. A few online services are fixing the ambiguities, also called PPP with Ambiguity Resolution (PPP-AR) PPP-AR solutions, while most of them solve ambiguities as a float. CSRS-PPP has provided solutions as PPP-Float until October 20th, 2020. After this date, the CSRS-PPP system upgraded to CSRSPPP-Ambiguity Resolution (PPP-AR), and solutions were produced by fixing the GPS ambiguities based on the decoupled clock model (DCM) for the data collected after January 1st, 2018 [31]. Our field measurements were collected before 2018, so they were processed using CSRS-PPP solutions.

The mathematical modeling equation of PPP of pseudo range and carrier phase observations is shown in Equations (2) and (3) [32]:

$$l_p = \rho + c(dt - dT) + M\ ztd + \varepsilon_p \tag{2}$$

$$l_\phi = \rho + c(dt - dT) + M\ ztd + N\lambda + \varepsilon_\phi \tag{3}$$

where:

l_P (Pseudo-range observation): Is the ionosphere-free combination of the L1 and L2 pseudo ranges (2.54P1–1.54P2);

l_ϕ (Carrier phase observation): Is the ionosphere-free combination of L1 and L2 carrier phases (2.54ϕ1–1.54ϕ2);

ρ (Geometric range): Is the geometrical range computed as a function of satellite and station coordinates;

c (Speed of light): Is the constant speed at which electromagnetic signals travel in a vacuum (~299,792,458 m/s);

dt (Receiver clock bias): Is the station clock offset from GPS time;
dT (Satellite clock bias): Is the satellite clock offset from GPS time;
M (Mapping function): Is a function to map tropospheric from slant to zenith;
ZTD (Zenith Tropospheric Delay): is the tropospheric zenith total delay due to the neutral atmosphere, wavelength, and ionosphere-free combination. The tropospheric delay is the sum of the wet and hydrostatic parts.
λ (Carrier wavelength): Is the carrier or carrier combination, wavelength;
N (Integer ambiguity): Is the unknown number of full carrier phase cycles between the satellite and receiver, critical for high-precision positioning;
εP Measurement noise and unmodeled errors in pseudo-range observation (m);
εP Measurement noise and unmodeled errors in carrier phase observation (m).

3. Material and results

3.1. Study area and measurements

The selected area of this research is placed alongside the Mediterranean Sea coast zone located in the northern region of Egypt, as shown in **Figure 2**. The area is confined between Al Burullus city at a longitude of 30°57′51″ and Rosetta city at E30°23′18″ with about 60 km of longitudinal length and an average of 0.5 km perpendicular to the coastal line. It covers an approximate area of 39 km^2. The selection of this region is due to the increasing necessity for development activities to prevent shorelines from erosion induced by global warming. So, a topographic map with high accuracy was required by ECPA for determining the best locations of protection works along the area continuously. This map was produced by the Survey Research Institute [33]. Static and kinematic GPS observations, in addition to leveling measurements, were collected and discussed by [4]. A brief discussion about these measurements is presented in the following sections.

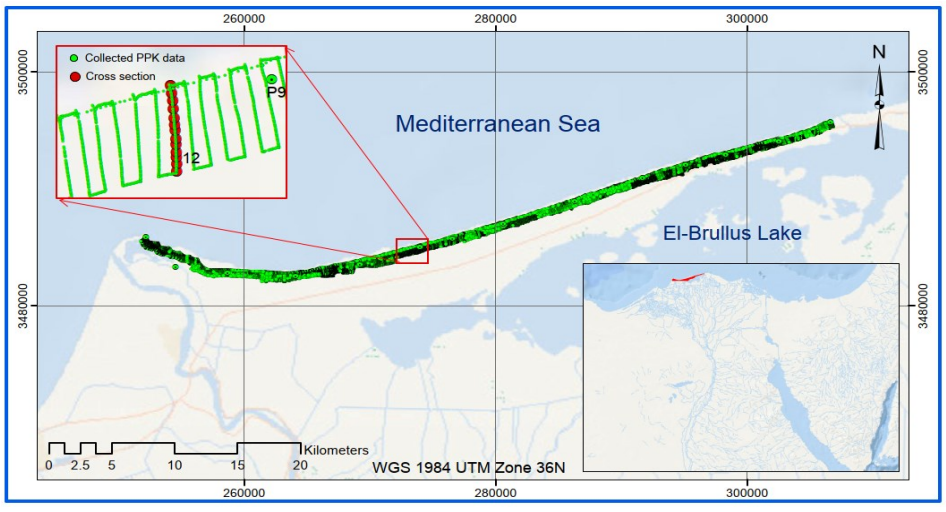

Figure 2. The study area with a part of kinematic measurements.

3.1.1. Static GPS observations

As a result of the scarcity of reference points throughout many coastal regions, it was important to establish a new permanent reference point to cover all the study area

for current and future required measurements. Fourteen control points were installed across the study area, as shown in **Figure 3**, with an approximate spacing of 5 km. This distance was determined based on the terrain characteristics to ensure optimal positioning accuracy. The chosen separation was specifically selected to account for geoid undulation variations within the study area, as the collected measurements were intended to develop a methodology for generating topographic contour maps using the post-processed kinematic differential GPS technique (PPK-GPS) [4]. To achieve the required accuracy, the selected spacing was carefully considered; however, it may vary depending on specific surveying requirements and the terrain conditions of the investigated area. To ensure sustainability of these points for future works, a cub-shaped concrete structure with upper dimensions of 40 × 40 cm and lower dimensions of 50 × 50 cm was built with a total height of 1 m divided into equal parts over and underground as shown in **Figure 4**. A metal cap with a 10 cm steel rod fixed above the concrete for the observation process.

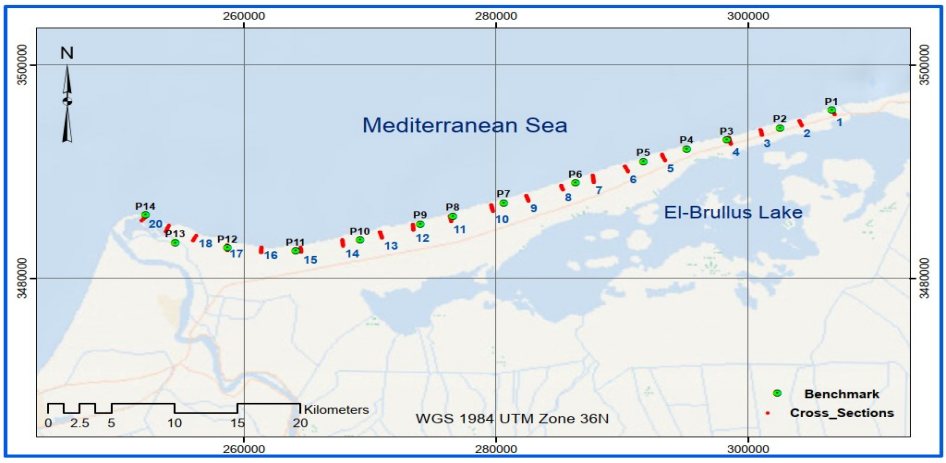

Figure 3. Location of control stations and check cross sections along the study area.

To calculate the accurate 3-D coordinates of these established 14 control points, static GPS observations were performed with occupation times ranging from 2 to 3 hours. They were linked with the nearest two first-order triangulation points of the Egyptian Surveying Authority (ESA) to be solved as an over-constrained network [34]. Observations were collected using 4 dual-frequency 5700 Trimble receivers and processed using Trimble Business Center Software (TBC). The precise ephemeris was used to enhance the accuracy of the estimated coordinates. The required horizontal and vertical precisions of ± (2 cm + 1 ppm) and (± 5 cm + 1 ppm) were achieved for all points. The network was adjusted relative to the International Terrestrial Reference Frame (ITRF) system at 2014 epochs according to the measurement date.

To address GPS measurement challenges related to signal interference and multipath effects, various strategies can be implemented. Utilizing high-quality GNSS receivers, interference-resistant antennas, and avoiding electronic interference sources helps reduce signal disruptions. In our coastal study area, multipath effects were negligible due to the open-sky environment. Furthermore, to achieve optimal accuracy and minimize errors, appropriate observation timing, the use of PPK observation methods (stop and go mode), and post-processing techniques were applied.

Figure 4. Two photos of the established control stations.

3.1.2. Kinematic measurements

To create an accurate topographic map for the study area using GPS observations, the Post-Processed Kinematic (PPK) method and Stop and Go mode were adopted for collecting data. During kinematic observations, one receiver occupied the nearest reference station as a base, and 2 other receivers were used as rovers. The area was divided into parallel cross-sections perpendicular to the seacoast line with 100 m separated distances between each cross-section, as shown in **Figure 2**. The cross-sections varied in length between 0.4 and 0.6 km. The average space between observed points using stop and go modes is 10 m. All data were then processed using TBC software to estimate the accurate 3-D coordinates. The cross-sections point average accuracy was (1.2 cm) and (2.4 cm) for HZ and VL positions, respectively. Twenty of these cross-sections with a spacing of approximately 3 km, as shown in **Figure 3,** were selected to be compared with their solution results obtained using CSRS-PPP service. The main purpose of these twenty cross-sections during measurements is to be observed using PPK modes and also leveling methods to fairly judge the achieved precision of producing topographic maps using PPP methods as discussed by [4].

3.1.3. PPP static and kinematic results

The main objective of this study is to evaluate the CSRS-PPP service accuracy for static and kinematic measurements. So, after solving these measurements using relative positioning techniques and estimating the final processed accurate 3-D coordinates using TBC software. Static and kinematic raw data observations were uploaded to the CSRS-PPP online website [29] for solutions. The website accepts only Receiver Independent Exchange format (RINEX) for static and kinematic data. Users must manually upload RINEX files, and large datasets may take longer to process, making them less convenient for high-frequency or large-scale GNSS campaigns. Users can't upload any other format, and they have to convert their observation files format into RINEX format for uploading, where any errors in formatting can lead to processing failures without clear troubleshooting guidance. Users are able to upload multiple RINEX files in a single (zip) or (tar) archive. An error email from the service may be received due to various reasons, such as duplicated data blocks in the submitted RINEX observation file at one or more epochs, and they must be corrected by

resubmitting the file for processing. Also, an insufficient number of epochs and observed satellites may cause failure in processing the file.

The reference system for the software is based on ITRF 2014 (epoch 2014 according to measurement date); the obtained coordinates have Cartesian XYZ format and Ellipsoidal and UTM (Universal Transverse Mercator) system zone 36 [29]. A PDF report was received via user email after about 2 min of uploading data. The PDF report is about five pages, including solution results, final coordinates, and several plots showing ambiguity status, tracked satellite, and pseudo-range and carrier phase residuals. We should conclude that the received PDF report from the CSRS-PPP service has several limitations, including a lack of in-depth error analysis, such as multipath effects, atmospheric delays, and satellite geometry limitations. It provides general accuracy estimates but lacks detailed statistical analyses or confidence intervals for positioning errors. After receiving CSRS-PPP solutions, their estimated results for both static and kinematic measurements were compared with results that were obtained using the relative positioning solution. **Figure 5** displays a flowchart of the study methodology.

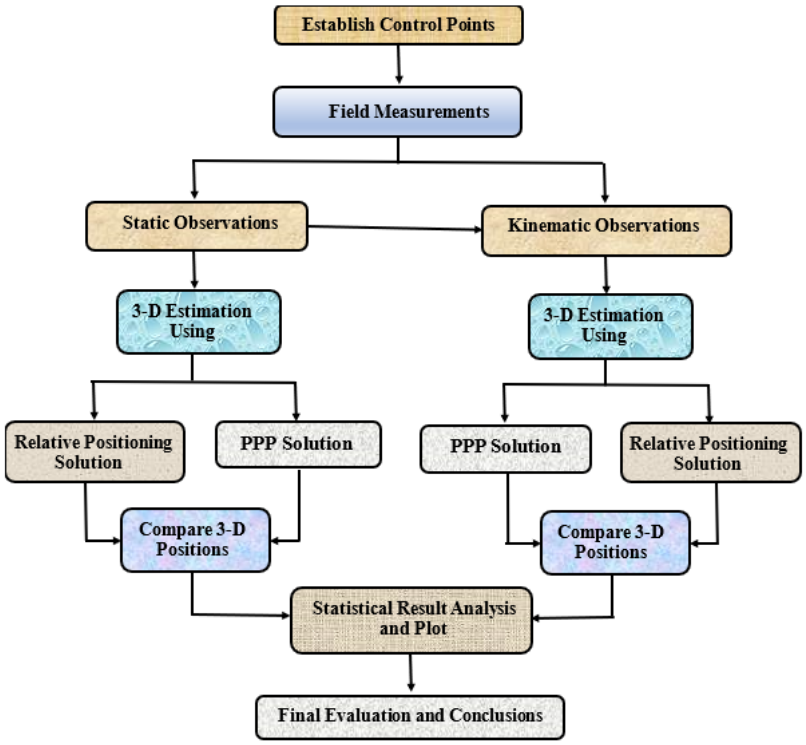

Figure 5. Flowchart of the study methodology.

3.2. Results

3.2.1. Static results

Table 1 shows the differences between coordinates obtained from static PPP and relative positioning solutions for the 14 control points, and **Table 2** represents the summary of statistics, maximum, minimum, RMS, median, and NMAD for these differences. **Figure 6** shows the violin plots of results. The computed values of Normalized Median Absolute Deviation (NMAD) and violin plots were used to

acquire a better understanding of differences, detect outliers, and emphasize data peaks. As seen from the results, the difference of 2D position reaches 2.1 cm and 2.5 cm as a maximum value with RMSE values of 1.2 cm and 1.4 cm for both East and North, respectively. While the height component differences range between −5.9 and 11.3 cm with an RMSE value of 9.1 cm.

Table 1. Differences between static CSRS-PPP and relative positioning solutions of control stations.

point ID	ΔN	ΔE	ΔH
P1	0.018	−0.017	0.081
P2	−0.004	0.007	0.1
P3	0.008	−0.017	0.059
P4	−0.007	0.010	0.108
P5	0.000	−0.005	0.074
P6	−0.001	−0.014	0.083
P7	−0.020	0.011	0.094
P8	0.025	0.008	0.078
P9	−0.005	0.011	0.113
P10	−0.009	0.013	0.085
P11	0.020	0.021	0.096
P12	0.016	−0.006	0.089
P13	0.004	0.012	0.104
P14	−0.016	−0.002	0.099

Table 2. Differences in statistics between static CSRS-PPP and relative positioning solutions of control stations.

	Min	Max	RMSE	Median	NMAD
ΔE	−0.017	0.021	0.012	0.007	0.012
ΔN	−0.02	0.025	0.014	−0.001	0.010
ΔH	−0.113	−0.059	0.091	−0.091	0.011

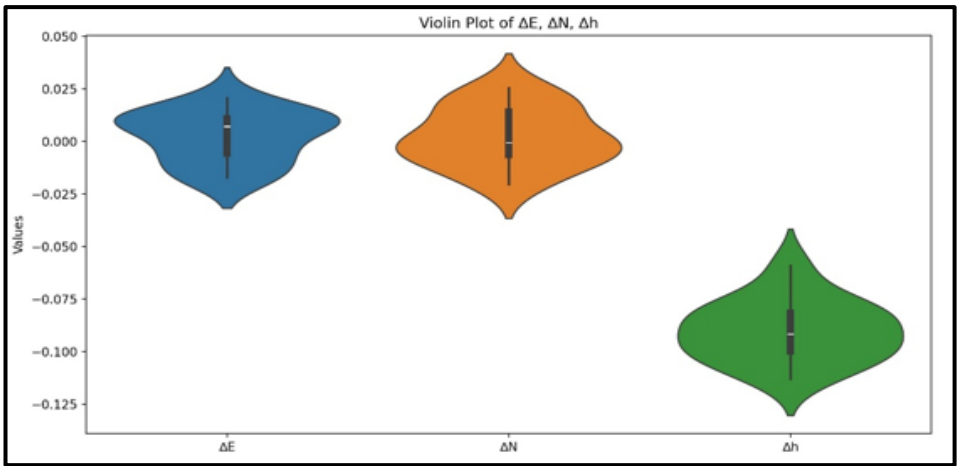

Figure 6. Violin plots of the difference of the static CSRS-PPP solution.

3.2.2. Kinematic results

As mentioned before, the twenty cross-sections of kinematic observations were solved using both CSRS-PPP and relative positioning. The average horizontal and vertical GPS positioning uncertainties for each cross-section point are provided in **Table 3**.

Table 3. The average HZ and VL precision for the 20 check cross-sections.

Sec	HZ. Precision (m)	VL. Precision (m)	Sec	HZ. Precision (m)	VL. Precision (m)
1	0.012	0.022	11	0.014	0.031
2	0.011	0.017	12	0.012	0.022
3	0.011	0.018	13	0.010	0.014
4	0.015	0.029	14	0.010	0.019
5	0.012	0.022	15	0.014	0.024
6	0.014	0.023	16	0.010	0.019
7	0.014	0.029	17	0.014	0.023
8	0.013	0.028	18	0.011	0.020
9	0.015	0.037	19	0.011	0.017
10	0.015	0.032	20	0.014	0.020

Table 4 shows the statistics summary of the differences between two solution results for 2D position and height components and **Figure 7a,b** represents graphically the absolute differences for 2D position and height components respectively. **Figure 8** shows the median values of ΔE, ΔN, and Δh for all cross sections.

Table 4. Statistics values for kinematic measurement differences of the twenty cross-sections.

Min Max Median RMSE	**SEC.1**	**SEC.2**	**SEC.3**	**SEC.4**	**SEC.5**	**SEC.6**	**SEC.7**	**SEC.8**	**SEC.9**	**SEC.10**
ΔN	−0.035 0.030 −0.003 0.021	−0.038 0.014 −0.017 0.021	−0.046 0.007 −0.022 0.026	−0.036 0.020 −0.019 0.022	−0.036 0.000 −0.020 0.024	−0.028 0.012 −0.017 0.019	−0.029 0.001 −0.017 0.017	−0.014 0.004 −0.006 0.007	−0.030 −0.010 −0.022 0.023	−0.020 0.005 −0.005 0.010
ΔE	−0.044 0.014 −0.006 0.022	−0.049 0.026 −0.006 0.018	−0.011 0.030 0.005 0.012	−0.040 0.008 −0.015 0.021	−0.031 0.000 −0.016 0.019	−0.049 −0.022 −0.034 0.034	−0.047 −0.021 −0.037 0.037	−0.048 −0.030 −0.036 0.037	−0.041 −0.011 −0.032 0.031	−0.050 −0.034 −0.043 0.043
Δh	−0.125 −0.046 −0.096 0.094	−0.184 −0.092 −0.122 0.133	−0.141 −0.065 −0.102 0.104	−0.096 −0.045 −0.073 0.070	−0.106 −0.036 −0.071 0.073	−0.142 −0.084 −0.112 0.114	−0.121 −0.093 −0.108 0.106	−0.109 −0.079 −0.099 0.098	−0.141 −0.067 −0.102 0.107	−0.168 −0.102 −0.124 0.130
Min Max Median RMSE	**SEC.11**	**SEC.12**	**SEC.13**	**SEC.14**	**SEC.15**	**SEC.16**	**SEC.17**	**SEC.18**	**SEC.19**	**SEC.20**
ΔN	−0.050 0.012 −0.016 0.026	−0.036 −0.003 −0.019 0.021	−0.045 0.044 −0.004 0.023	−0.042 0.041 −0.011 0.026	−0.040 0.032 −0.018 0.028	−0.042 0.032 −0.030 0.029	−0.030 0.039 −0.009 0.021	−0.047 0.043 −0.012 0.028	−0.037 0.021 −0.009 0.018	−0.043 0.005 −0.020 0.025

Table 4. (*Continued*).

Min Max Median RMSE	SEC.11	SEC.12	SEC.13	SEC.14	SEC.15	SEC.16	SEC.17	SEC.18	SEC.19	SEC.20
ΔE	−0.032 0.007 −0.016 0.017	−0.037 −0.003 −0.021 0.021	−0.044 0.038 −0.018 0.026	−0.047 0.034 −0.021 0.028	−0.037 0.036 −0.006 0.024	−0.034 0.030 0.010 0.020	−0.041 0.047 −0.016 0.029	−0.036 0.030 −0.003 0.022	−0.036 −0.002 −0.015 0.021	−0.030 0.037 −0.015 0.021
Δh	−0.128 −0.095 −0.110 0.112	−0.173 −0.115 −0.143 0.146	−0.129 −0.082 −0.097 0.103	−0.128 −0.051 −0.089 0.098	−0.173 −0.072 −0.108 0.124	−0.138 −0.067 −0.118 0.115	−0.162 −0.074 −0.110 0.116	−0.150 −0.070 −0.111 0.113	−0.135 −0.071 −0.097 0.105	−0.151 −0.067 −0.113 0.113

We can notice from the table a considerable variation in Δh cross-sections, indicating that height difference is more variable than ΔE and ΔN. As shown in the figure, the 2D position differences have a maximum value of 5 cm or better with an average median of 3.5 cm and RMSE of 3.4 cm for all cross-section points. While differences of height components fall within the range between values of 3.6 cm and 18.4 cm with an RMSE value of 10.9 cm.

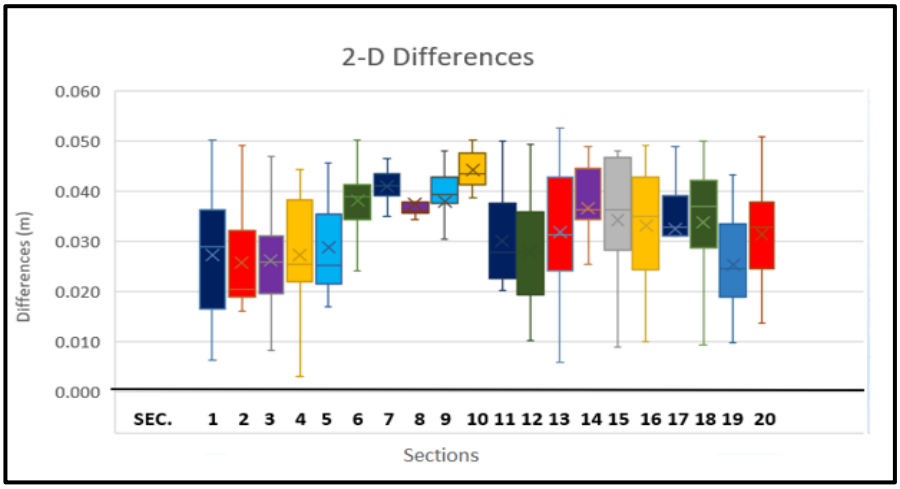

(a) Box plot for all cross-sections of height component.

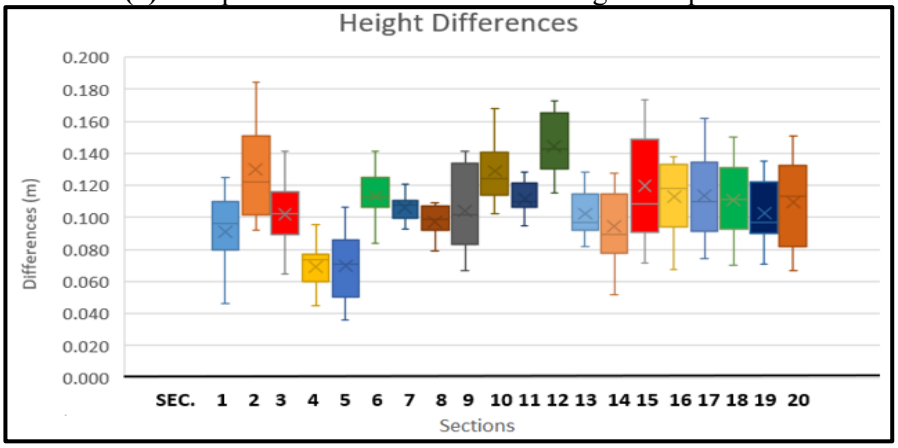

(b) Box plot for all cross-sections of 2D positions.

Figure 7. Box plots for all cross-sections of both 2D and height components.

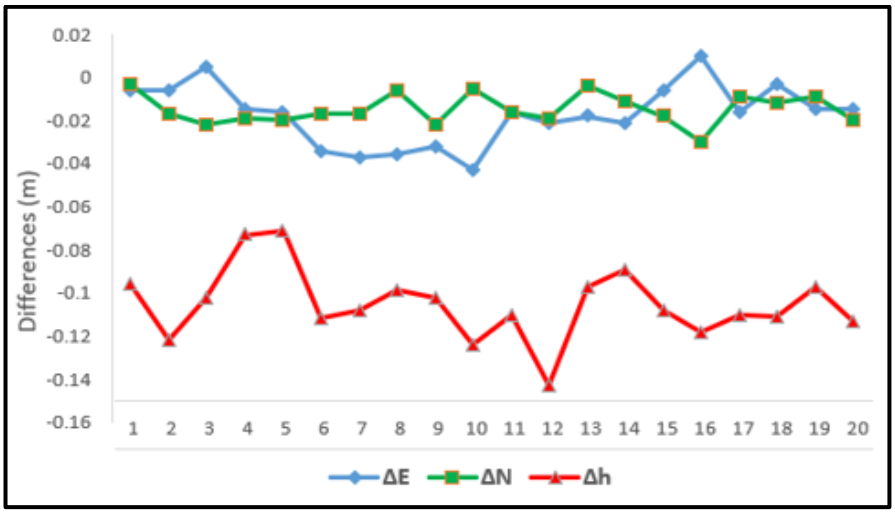

Figure 8. Median values for all cross sections.

4. Discussion

The main objective of this research is to evaluate the estimated accuracy of PPP solutions for post-processed kinematic observations using the CSRS-PPP service. The use of the PPP technique spread rapidly in many fields and applications as a result of its simplicity, cost-effectiveness, and acceptable accuracy. Field static and kinematic observations were collected and solved using both relative positioning and PPP techniques, and their results were compared to fairly evaluate the obtained accuracy. According to the obtained results, the outfinding proved that PPP service is an efficient method in static mode, especially for horizontal positioning, where the differences were less than 2.54 cm. However, PPP achieves a lower accuracy for the height component with a height difference of up to 11.3 cm. For kinematic mode, the achieved horizontal accuracy was judged satisfactory with a higher discrepancy of 4.7 cm. But in the height component accuracy, it was not satisfied because the differences reached up to 18.4 cm, and these values may not be suited for a variety of applications that require the highest accuracy.

Vertical accuracy in PPP is generally lower than horizontal accuracy due to various limitations in GNSS positioning and error modeling. Factors such as poor satellite geometry due to fewer observed satellites, tropospheric and ionospheric delays, and multipath effects, particularly in urban areas, degraded vertical accuracy. Additionally, long convergence times and inaccuracies in atmospheric corrections and satellite orbit data further reduce accuracy and precision. In our measurements, good satellite geometry with sufficient available satellites and an open-sky environment with minimal multipath were achieved. However, the primary causes of larger elevation errors are ionospheric delays, satellite orbital errors, and atmospheric modeling limitations. The accuracy achieved by the kinematic PPP solution can be suitable for various applications requiring movement-based measurements, practically in open areas. However, its reliability decreases in urban environments and forested regions. Additionally, it isn't suitable for applications that demand immediate results.

5. Conclusion

The extensive improvement of modern technology had a significant impact on all fields and led to the development of new approaches. Several new positioning techniques and methods were developed in surveying and geodesy fields. The main concern in the developed techniques is to decrease the fieldwork and minimize the cost and time of works. However, these modern techniques should achieve a suitable accuracy. One of the most popular modern positioning techniques is PPP, or single point positioning, with no need for reference or base stations. In this study we evaluate the accuracy of the CSRS-PPP solution in both static and kinematic modes using field measurements. Solutions derived from CSRS-PPP were compared with those estimated from relative positioning techniques.

Based on the results, the CSRS-PPP technique could be used for the solution of static measurements as an alternative method to the relative positioning technique. PPP achieves a suitable accuracy, especially in horizontal positions, for several applications and fields, and about 11.3 cm height level accuracy is obtained by the CSRS-PPP solution. For the kinematic mode, CSRS-PPP provides us with an accuracy of ± 5 cm for 2D positions and approximately 18.4 cm or better for height components. The achieved 2D position accuracy is considered acceptable for most moving measurement environmental applications. However, height accuracy may not be suitable for many applications. It should be noted that PPP may not be suitable for several applications that require immediate results. PPP accuracy is affected by multipath errors and atmospheric conditions, making it less reliable in urban areas, forests, and coastal regions with frequent signal interference. Unlike RTK, which can resolve integer ambiguities quickly using local base stations, PPP often relies on float solutions (PPP-Float) or slower ambiguity resolution techniques (PPP-AR), affecting rapid positioning needs.

Further work is required for improving the accuracy of height components via kinematic PPP to fulfill other applications that require higher accuracy and should be investigated. This improvement of PPP-derived heights may be achieved by integrating with ground station corrections, multi-frequency PPP, INS (Inertial Navigation Systems) integration, advanced tropospheric models, and the use of machine learning for error modeling. Various PPP services that offer kinematic solutions should be examined and compared with the results of this study. Additionally, modern PPP algorithms, such as PPP-AR and PPP-Float, should be analyzed and discussed. Additionally, the impact of the region's diverse geographical environment and climatic conditions on measurement accuracy should be thoroughly examined.

Funding: This research work was funded by Institutional Fund Projects under grant No. (IFPIP-1238-137-1443).

Acknowledgment: The authors gratefully acknowledge technical and financial support provided by the Ministry of Education and King Abdulaziz University, DSR, Jeddah, Saudi Arabia.

Data availability: The data used in this study were obtained from the corresponding author upon reasonable request.

Conflict of interest: The author declares no conflict of interest.

References

1. ElShouny AF. The combined adjustment of terrestrial and satellite control network [Master's thesis]. Minoufiya University; 2008.
2. Xu G. GPS: Theory, Algorithms and Applications, 2nd ed. Springer; 2007. ISBN 978-3-642-09181-0.
3. Leick A. GPS Satellite Surveying. Wiley; 1990.
4. El Shouny A, Nagy Y, Magdy H. Evaluating the performance of using PPK-GPS technique in producing topographic contour map. Marine Geodesy. 2017; 40(4): 224–238.
5. Liu R, Guo B, Zhang A, Yimwadsana B. Research on GPS precise point positioning algorithm with a Sea Surface Height Constraint. Ocean Engineering. 2020; 197: 106826.
6. El-Mowafy A. Precise real-time positioning using Network RTK. Global Navigation Satellite Systems: Signal, Theory and Applications. 2012; 7: 161–188.
7. Wanninger L. Virtual Reference Stations (VRS). GPS Solution. 2003: 7: 143–144.
8. Dardanelli G, Maltese A, Pipitone C, et al. NRK, PPP or static, that is, the question. Testing different positioning solutions for GNSS survey. Remote Sensing. 2021; 13(7): 1406.
9. Zumberge JF, Heflin MB, Jefferson DC, et al. Precise point positioning for the efficient and robust analysis of GPS data from large networks. Journal of Geophysical Research. 1997; 102(B3): 5005–5017.
10. Dawidowicz K, Krzan G. Coordinate estimation accuracy of static Precise Point Positioning using online PPP service: A case study. Acta Geodaetica et Geophysica. 2014; 49: 37–55.
11. El-Mowafy A. Analysis of Web-Based GNSS Post-Processing Services for Static and Kinematic Positioning Using Short Data Spans. Survey Review. 2011; 43: 535–549.
12. Gandolfi S, Tavasci L, Poluzzi L. Study on GPS–PPP Precision for Short Observation Sessions. GPS Solut. 2017; 21: 887–896.
13. Ge Y, Cao X, Lyu D, et al. An investigation of PPP time transfer via BDS-3 PPP-B2b service. GPS Solutions. 2023; 27(2): 61.
14. Guo Q. Precision comparison and analysis of four online free PPP services in static positioning and tropospheric delay estimation. GPS Solutions. 2015; 19(4): 537–544.
15. Martín Furones ÁE, Anquela Julián AB, Berné Valero JL, Sanmartin M. Kinematic GNSS-PPP results from various software packages and raw data configurations. Scientific Research and Essays. 2012; 7(3): 419–431.
16. Anquela AB, Martín A, Berné JL, Padín J. Gps and Glonass Static and Kinematic PPP Results. J. Surv. Eng. 2013; 139: 47–58.
17. Abdallah A, Schwieger V. Kinematic Precise Point Positioning (PPP) Solution for Hydrographic Applications. In: Proceedings of the FIG Working Week May 2015 from the Wisdom of the Ages to the Challenges of the Modern World; Sofia, Bulgaria; 17–21 May 2015.
18. Alkan RM, Ozulu İM, Ilci V. Precise Point Positioning (PPP) technique versus network-RTK GNSS. FIG Working Week. 2016; 2016: 1–10.
19. DeSanto JB, Chadwell CD, Sandwell DT. Kinematic post-processing of ship navigation data using precise point positioning. Journal of Navigation. 2019; 72(3): 795–804.
20. Yang FX, Zhao L, Li L, et al. Performance evaluation of kinematic BDS/GNSS real-time precise point positioning for maritime positioning. Journal of Navigation. 2019; 72(1): 34–52.
21. ElShouny A, Miky Y. Accuracy assessment of relative and precise point-positioning online GPS processing services. Journal of Applied Geodesy. 2019: 13(3): 215–227.
22. Bulbul S, Bilgen B, Inal C. The performance assessment of Precise Point Positioning (PPP) under various observation conditions. Measurement. 2021; 171: 108780.
23. Mendez Astudillo J, Lau L, Tang YT, Moore T. Analyzing the Zenith Tropospheric Delay Estimates in online precise point Positioning (PPP) Services and PPP Software Packages. Sensors. 2018; 18: 580. doi: 10.3390/s18020580

24. Heo Y, Li B, Lim S, Rizos C. Development of a network real-time kinematic processing platform. In: Proceedings of the 22nd International Technical Meeting of Satellite Division of the Institute of Navigation (ION GNSS 2009); Savannah, GA, USA; 22–25 September 2009.
25. Lachapelle G, Cannon ME, Lu G. High Precision GPS Navigation with Emphasis on Carrier Phase Ambiguity Resolution. Marine Geodesy. 1992; 15: 253–269.
26. Al Shouny A, Kamel A, Miky Y. Kinematic precise point positioning heights enhancement using static measurements and Voronoi's corrector surface. International Journal of Digital Earth. 2024; 17(1): 2327843.
27. Alkan RM, Saka MH, Ozulu İM, İlçi V. Kinematic precise point positioning using GPS and GLONASS measurements in marine environments. Measurement. 2017; 109: 36–43.
28. Mireault Y, Tétreault P, Lahaye F, et al. Online Precise Point Positioning: A New, Timely Service from Natural Resources Canada. GPS World. 2008; 19(9): 59–64.
29. Natural Resources Canada. Precise Point Positioning. Available online: http://www.nrcan.gc.ca/earth-sciences/geomatics/geodetic-referencesystems/tools-applications/10925#ppp (accessed on 2 December 2022).
30. Tétreault P, Kouba J, Héroux P, Legree P. CSRS-PPP: An internet service for GPS user access to the Canadian spatial reference frame. Geomatica. 2005; 5 (1): 17–28.
31. Mutlu B, Erol S, Alkan RM. The performance analysis of the post-mission web-based static and kinematic PPP-AR service. Rudarsko-Geološko-Naftni Zbornik. 2023; 38(4): 103–116.
32. Heroux P, Kouba J. GPS precise point positioning using IGS orbit products. Phys. Chem. Earth. 2001; 26: 573–578
33. Survey Research Institute (SRI) Technical Report. The technical report of the survey work performed for the area between Rosetta and El-Brullus as part of the project adaptation of the Nile Delta to climatic changes and sea water rise. NWRC; 2014.
34. Sobeih MF, Doma MI, El Shoney AF. Mixture-Order Design of GPS Networks Based on Genetic algorithms. ERJ Engineering Research Journal. 2010; 33(4): 431–439.